Nat Hazards (2014) 74:251–268
DOI 10.1007/s11069-014-1205-5

ORIGINAL PAPER

The Dwarskersbos, South Africa local tsunami of August 27, 1969: field survey and simulation as a meteorological event

Emile A. Okal · Johan N. J. Visser · Coenraad H. de Beer

Received: 24 December 2013 / Accepted: 21 April 2014 / Published online: 21 May 2014

Abstract We investigate the hitherto unexplained wave which inundated the village of Dwarskersbos, South Africa, in the early hours of August 27, 1969, in the absence of any seismic disturbance or major meteorological storm. A field survey, based on the interview of nine elderly witnesses still residing in the community, documented maximum run-up of 2.9 m, concentrated on an extremely short segment of coastline, less than 2 km in length. These characteristics are incompatible with generation by a seismic source (which, at any rate, should have been felt by the population). A landslide source, located at the only canyon featuring a steep enough ocean floor, is also ruled out since a numerical simulation fails to reproduce the concentration of the wave at Dwarskersbos. By contrast, the wave can be explained as a "meteo-tsunami" resulting from resonance between a meteorological squall propagating at 18 m/s in the azimuth N101°E and a gravity wave propagating in the shallow waters off the eastern shore of St. Helena Bay. This is confirmed by numerical simulation under the formalism of Proudman (Dynamical oceanography. Methuen, London, 1953), which provides a satisfactory model of the distribution of run-up along the beach.

1 Introduction

In the early morning hours of Wednesday, August 27, 1969, a small segment of the Atlantic coast of the Western Cape Province, South Africa, was attacked by a wave which flooded a number of houses in the community of Dwarskersbos, approximately 160 km

E. A. Okal (✉)
Department of Earth and Planetary Sciences, Northwestern University, Evanston, IL 60208, USA
e-mail: emile@earth.northwestern.edu

J. N. J. Visser
10 Papawer Street, Dwarskersbos, Velddrif 7365, South Africa

C. H. de Beer
Council of Geoscience, P.O. Box 572, Bellville 7535, South Africa

north of Cape Town (Fig. 1). While no human victims were deplored, this small tsunami resulted in significant structural damage to the local bathing house (mainly from its backflow cutting through a prominent gulley), and in the loss of light boats and poultry.

The origin of the wave has remained an enigma among the tsunami community for several decades. We present here the results of a field survey conducted 41 years after the event, in the form of a database built along the standards of modern-day post-tsunami surveys (Synolakis and Okal 2005), and of a hydrodynamic simulation suggesting that the phenomenon was meteorological in origin.

The community of Dwarskersbos is located on the eastern side of St. Helena Bay. The latter constitutes a broad embayment, limited to the north by the Bobbejaansberg promontory at Elands Bay, and to the south by the large Sandy Point headland and promontory. The eastern coastline is essentially linear, with a radius of curvature of the shore line in excess of 45 km.

Dwarskersbos is the only built-up community between Elands Bay, 43 km to the north and Velddrif, 13 km to the south at the mouth of the Berg River, where the coast bends sharply west to link up with the West Coast Peninsula, ending at the Shelley Point promontory. In 1969, Dwarskersbos was mainly an informal fishing community, and a holiday resort for the inland farmers, located on private land. Its development was minimal, with no electricity or running water; most houses had mainly two rooms. Its population was approximately 150. It has now been developed considerably, with 17 streets labeled alphabetically from A to R opened perpendicular to the shoreline at intervals averaging 75 m, a caravan park and a large extension to the north. However, some of the original dwellings still stand, most of them improved through the addition of several rooms, and a number of 1969 residents still live in the same houses. Most of these dwellings were aligned northwest–southeast and were built on elevated ground formed by low amplitude dunes.

The built-up areas were separated from the sea by a wide stretch of mildly vegetated sand dunes, whose width varies from 40 to 150 m; their morphology has reportedly changed in the past 40 years, but the present location of the shoreline and the altitude of the built-up areas have remained more or less constant.

2 The tsunami

The timing of the tsunami can be asserted as Wednesday, August 27, 1969, around 03:30 to 04:00 SAST (01:30–02:00 GMT). This date was confirmed by most of our witnesses, with the exception of one family who would put the event on the 26th. We prefer the date of the 27th, given that it was reported in the late edition of the Cape Town newspaper *Cape Argus*, published around 5 p.m. on the 27th, as having occurred the same morning, and in the edition dated on the 28th of the morning newspaper *Cape Times*, as having occurred the previous day.

The nighttime occurrence of the wave means that there were no direct witnesses of its propagation from the beach to the community. Rather, residents were awakened by the flooding of their houses and in turn woke up neighbors whose houses were further inland. Also, a fraction of the population was fishing at sea.

3 Survey

Our methodology follows that of previous surveys of historical tsunamis, such as the Aleutian event of 1946 (Okal et al. 2002) and the 1956 Amorgos tsunami in Greece (Okal

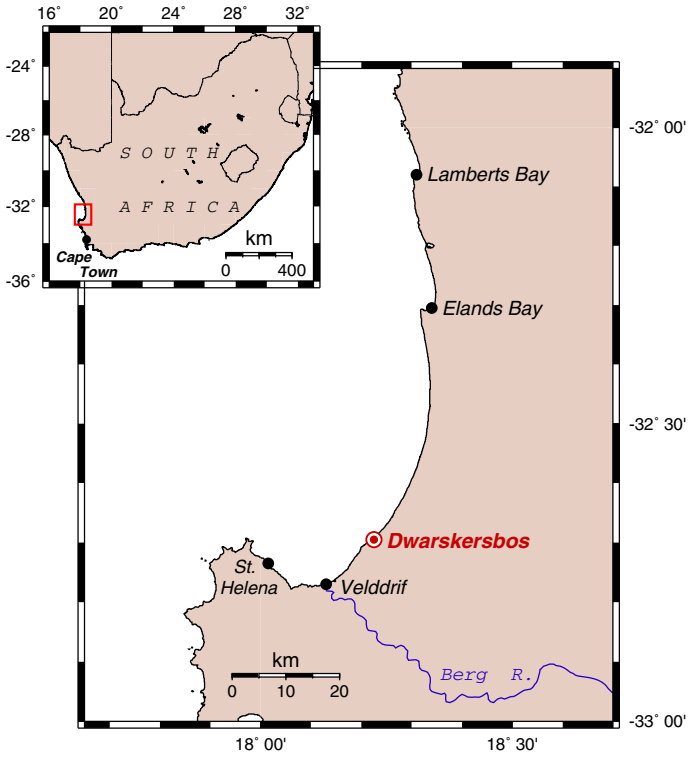

Fig. 1 Map of the study area. The insert at *top left* locates the main map (*box*) within South Africa

et al. 2009). They consist of identifying elderly witnesses of the event, recording their testimony, and using standard surveying techniques to obtain a quantitative database of the wave's penetration, based on their recollections.

We recall that *inundation* is defined as the horizontal distance from the shoreline of maximum penetration of the wave; *run-up* is the altitude above sea level of the point of maximum penetration where inundation is measured; and *flow depth* the thickness of the water column during flooding, measured at a reference point between the shore line and the point of maximum penetration.

The field survey was conducted by the three authors on September 07–09, 2010. In the weeks preceding the survey, elderly witnesses still residing in Dwarskersbos were identified by Visser, who himself has retired in the community (but did not live there in 1969).

4 Results

We were able to identify and interview 9 witnesses of the 1969 tsunami, aged 25–42 at the time of the event (66–83 when interviewed), and still living in Dwarskersbos in 2010. They provided us with detailed descriptions of the flooding at 13 separate locations along the coastline. Results are compiled in Table 1 and Figs. 2 and 3.

Table 1 Surveyed dataset at Dwarskersbos and vicinity

Waypoint number	Present-day street	Coordinates at shoreline (°S; °E)	Date (2010) surveyed and Time (SAST)	Inundation (m)	Run-up (m)	Flow depth[a] (m)	Notes
Event of 27 August 1969							
Dwarskersbos							
101	Beyond R	32.68855 18.23551	07 SEP 10:10				Poephoek, House not reached, 160 m inland
102	P	32.69255 18.23138	07 SEP 12:10	260	2.85	1.00, 2.75. 124	Flooding reached maximum distance at present location of main road; Structural damage to bathing houses
103	I	32.69612 18.22711	07 SEP 12:50	85	0.55		House not flooded, 115 m form shore
104	J	32.69558 18.22791	07 SEP 13:00	106	1.5		Flooding reached just beyond present-day parking lot
105	A	32.69971 18.22161	07 SEP 10:55				Water did not reach Celba's cottage, 127 m from shore
106	F	32.69786 18.22433	07 SEP 16:00	173	1.6	0.75, 1.30, 77	Flow depth inside house
107	C	32.69933 18.22229	07 SEP 17:00	149	1.75	0.60, 1.60, 113	Intense flooding inside Eigelaar house
108	D	32.69797 18.22349	08 SEP 10:10	179	2.90		No water in house, 25–30 cm outside
109	FG	32.69750 18.22556	08 SEP 09:30	140	1.65		Water in house
110	NO	32.69365 18.23014	08 SEP 12:45	170	2.60		Water stopped just in front of Old School
111	D	32.69797 18.22349	08 SEP 10:10			1.10, 3.35, 123	Water in kitchen of Mostert's house
112	M	32.69414 18.22952	08 SEP 12:15	107	2.55	0.45, 2.10, 95	Liesbet Thiart's house; watermark on wall
Soverby							
113		32.71159 18.20430	07 SEP 10:30				Salt flats not reached at 50 m from shore
Event of 21 August 2008							
Saint Helena							
201		32.74125 18.01382	07 SEP 10:10	70	2.50		Shipworks, Port of St. Helena

Table 1 continued

Waypoint number	Present-day street	Coordinates at shoreline (°S; °E)	Date (2010) surveyed and Time (SAST)	Inundation (m)	Run-up (m)	Flow depth[a] (m)	Notes
202		32.77922 18.05188	09 SEP 11:25	25	2.55		Brandhuis, Johann Novella's house

[a] When listed, the three entries (in m) for flow depth are, respectively, the height of flow above ground, the elevation and the distance from shore of the flooded point

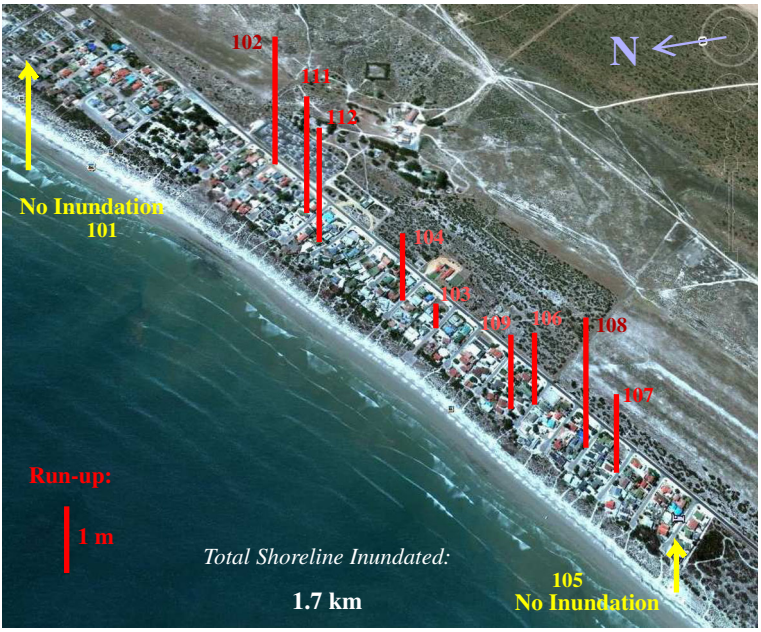

Fig. 2 Dataset listed in Table 1, superimposed on a Google-Earth view of Dwarskersbos. The *vertical bars* are scaled to run-up (*bar at left*), with their foot at the location of maximum inundation, as given by witnesses. Waypoint numbers refer to Table 1

In general, the water penetrated the area over an average inundation distance of 130 m. At one location (Waypoint 102, at the location of present-day Street P), the flooding reached a distance of more than 200 m, to the location of the present main road (which did not exist in 1969). The corresponding run-up heights range from less than 1 m at Street I to 2.9 m at Street N. The extent of inundation is rather irregular and reflects the variable, if mild, topography of the region and the network of sand tracks connecting the dwellings between themselves as well as with the public well (north of Street O; Fig. 3).

Our witnesses did not mention recurring waves, but rather a single episode of inundation. However, care has to be taken in interpreting their reports, as they were awakened by the flooding, which would not preclude the occurrence of precursory waves of smaller amplitude.

A remarkable aspect of our dataset is that the two extreme locations (Waypoints 101 to the northwest and 105 to the southeast) were not reached by the tsunami, even though they lie close to the berm, at distances from the shore generally inundated elsewhere in the

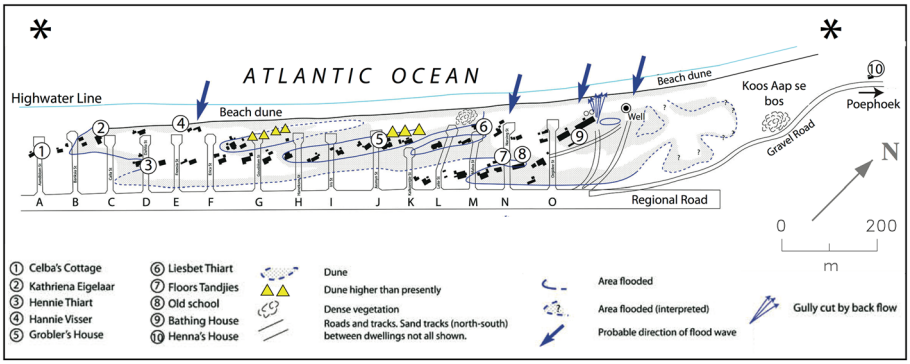

Fig. 3 Interpretation of the results of our survey. This map of Dwarskersbos is based on a 1967 Surveyor's map showing the proposed layout of the town once it is proclaimed. The houses present in the 1960s are shown as the *solid black blocks*. The extent of flooding is represented by the *dotted area enclosed by solid and dashed* (where only probable) lines. The *four solid arrows* indicate the inferred direction of arrival of the wave. The *large asterisks* indicate locations of Waypoints 101 and 105, where no inundation took place

village. In this framework, it is possible to derive the lateral extent of flooding of the wave, which was contained between the locations of present-day B and R Streets, a distance of only 1.7 km along the seafront. This pattern was confirmed by an additional data point (Waypoint 113) obtained at Soverby, the site of a fish processing industry during the 1930s and 1940s, 2.2 km southwest of Street A along the shore, where a witness stated that the 1969 wave did not reach the salt flats, located at an altitude of 2.15 m, and regularly inundated during major storms. It was also confirmed to us by witnesses that no evidence of flooding was reported in Velddrif, 13 km to the southwest, nor in Saint Helena, on the other side of the bay, where we interviewed a 74-year-old lifelong waterfront resident. Finally, we extended our investigations by interviewing three elderly lifelong residents of Elands Bay (43 km to the north of Dwarskersbos) and one in Lamberts Bay, 25 km farther north. Neither of them had witnessed any anomalous wave activity in 1969.

We thus come to the conclusion that the 1969 tsunami was spatially concentrated over a surprisingly short scale in the community of Dwarskersbos. The distribution of its run-up can be characterized by the dimensionless aspect ratio of its maximum amplitude to its half-width, $I_2 \approx 3 \times 10^{-3}$ in the formalism of Okal and Synolakis (2004). We note, however, that in the absence of populated settlements, our survey remains incomplete north of Dwarskersbos.

We attempted to gather additional scientific data potentially related to the Dwarskersbos tsunami of 1969. Unfortunately, we were unable to obtain any tide gauge data which may have been recorded in South Africa on that date. Regarding meteorological conditions on the night of the tsunami, most of our witnesses reported that it had been raining, with occasional lightning and thunder, but would not characterize this activity as exceptional in terms of intensity. While it was reported in the *Cape Argus* that atmospheric pressure measurements had shown significant fluctuations on the day of the tsunami, we were unable to find scientific meteorological data to quantitatively corroborate these descriptions.

5 The case of the 2008 event

Despite the exceptional character of the 1969 tsunami, other episodes of significant flooding, not directly attributable to extreme weather conditions, have been reported in the

same region. Among them, a 2008 episode at St. Helena stands out as the most recent and best documented such event.

Around 06:11 SAST (04:11 GMT) on Thursday, August 21, 2008, the port installations at St. Helena were flooded by a series of waves which inflicted significant damage, notably to the infrastructure of a shipyard, this phenomenon lasting for about 15 min. During our field survey of the 1969 tsunami, we visited St. Helena on September 08, 2010, interviewed witnesses of the 2008 event, and based on their testimony, measured a run-up of 2.5 m and an inundation of 70 m, as determined by the reported displacement of a small pick-up truck at the port of St. Helena. At Brandhuis, 5.5 km to the southeast, we obtained a run-up value of 2.55 m for a 20-m inundation from the testimony of a lifelong resident, who described two waves arriving "between 6 and 8 a.m."

Surprisingly, we were unable to document any observation in 2008 at Dwarskersbos, not only by our nine witnesses of the 1969 event, but also by the much larger community of present residents, which could be interpreted as indicating that the 2008 waves, if any, did not overtop the beach ridge separating the shore line from the built-up area.

On the other hand, Hartnady et al. (2009) documented instrumental observation of the 2008 waves by maregraphs over an 850-km stretch of coastline extending from Lüderitz, Namibia, in the north to Granger Bay near Cape Town in the south. These records show that the phenomenon lasted more than 24 h, with the largest amplitude matching the eyewitness observations of flooding and damage at St. Helena around 06:15 (GMT +2) on August 21. Based on the timing of the largest waves, Hartnady et al. (2009) proposed to locate the source of the main component of the tsunami around 28.5°S; 13.2°E, with an origin time of 23:00 GMT on August 20, 2008. Noting the presence of the Chamais Slump in the proposed source area, and the existence of documented gas hydrate structures in a structurally similar area 260 km to the southeast (Ben-Avraham et al. 2002), Hartnady et al. (2009) suggested to interpret the 2008 waves as due to a prolonged episode of slumping triggered by the destabilization of gas hydrates, and reaching its climax 24 h after it started. These authors also carried out a preliminary hydrodynamic simulation which quantitatively upheld the principal features of the four available maregrams.

However, Hartnady et al. (2009) noticed that barometric records at Port Nolloth showed signals inversely correlated with sea level residuals, speculating that while the ocean waves may have been driving the atmosphere, the opposite, i.e., a meteorological origin of the 2008 waves, might also be true [C. Hartnady, pers. comm., 2013].

Finally, during a northwestern storm in August 2012, the most extreme waves since 1977 were measured in the St. Helena Bay region [Royal Haskoning DHV, unpubl. rept., July 2013]. At Dwarskersbos, no flooding beyond the beach ridge was recorded, but extensive damage was caused at Soverby, where part of the lapa was washed away.

6 Interpretation: possible 1969 scenarios

Any interpretation of the 1969 Dwarskersbos event must somehow reconcile the significant amplitudes reached by the flooding, and its extreme spatial concentration, as well as the absence of any documented observation outside of Dwarskersbos.

6.1 Earthquake?

We first discount the possibility that the 1969 tsunami could have been generated by an earthquake. In the environment of an essentially rectilinear coastline such as the eastern

shore of St. Helena Bay, Okal and Synolakis (2004) have shown that one can use the "Plafker rule of thumb," which states that the maximum expectable run-up is at most twice the slip on the fault plane of a nearby parent earthquake. In the present case, the average run-up measured at 2.6 m would require more than 1 m of slip, which in turn, using Geller's (1976) scaling laws, would correspond to a moment of at least 3×10^{26} dyn*cm, or to conventional magnitudes $m_b \geq 6.0$; $M_s \geq 7$. This would be a stronger shock than, for example, the Ceres-Tulbagh earthquake, which occurred 32 days later, was widely felt, possibly as far as Johannesburg, caused extensive damage in the epicentral area (Keyser 1974) and was, obviously, recorded worldwide. No such event could be identified in the catalogs of the USGS or the ISC, nor was any earthquake felt in the region on the day of the tsunami.

In addition, a remarkable feature of our results is the extreme concentration of the flooding, which extends over no more than 1.7 km, suggesting an aspect ratio $I_2 \geq 3 \times 10^{-3}$, far in excess of those predicted by seismic scaling laws for an essentially linear coastline (Okal and Synolakis 2004).

6.2 Landslide?

Numerous examples of tsunamis locally generated by underwater landslides abound in the literature. Since such phenomena originate in the destabilization of landmasses in precarious equilibrium, they can be triggered by local earthquakes, as was the case for the 1998 Papua New Guinea disaster (Synolakis et al. 2002a), but can also occur occasionally in the absence of any perceived shaking, as in the case of the landslide of November 03, 1994, whose tsunami resulted in significant damage and one fatality in the port of Skagway, Alaska (Synolakis et al. 2002b). Because of the limited lateral dimension of landslides, their tsunamis can be concentrated over a small section of shoreline. Okal and Synolakis (2004) have proposed to use high values of the aspect ratio I_2 of the regional run-up distribution on a straight beach (in practice greater than 10^{-4}) as a proxy for establishing the generation of a tsunami by an underwater landslide. In this context, the value of I_2 at Dwarskersbos could in principle support this model.

6.2.1 Simulation

In order to test the possibility of a landslide source, we conducted a simulation for a potential scenario. We used a bathymetric grid from the Marine Geoscience Unit, which we interpolated to a step of 100 m (Fig. 4). It is noteworthy that most of St. Helena Bay, directly offshore from Dwarskersbos, is characterized by shallow bathymetry, and in particular by gentle slopes not exceeding 0.5 % (0.3°). In this context, and despite the presence of the nearby estuary of the Berg River, which could conceivably provide a source of gravitationally unstable sedimentary material, it is unlikely that a landslide could be generated directly along the eastern shore of St. Helena Bay. By contrast, an area 20 km to the northwest of Shelley Point promontory, around (32.6°S; 17.8°E), features a significant underwater canyon, where slopes can reach up to 3 % ($\sim 1.5°$). This canyon is apparently continuous from St. Helena Bay all the way to the edge of the continental shelf around (34°S, 17.2°E). Because of its relatively steep slopes, we select this location as the most probable source of a potential landslide in the vicinity of St. Helena Bay.

The source of our simulation uses the general landslide model proposed by Okal and Synolakis (2004) and utilized in the studies of the 1946 Aleutian and 1956 Amorgos

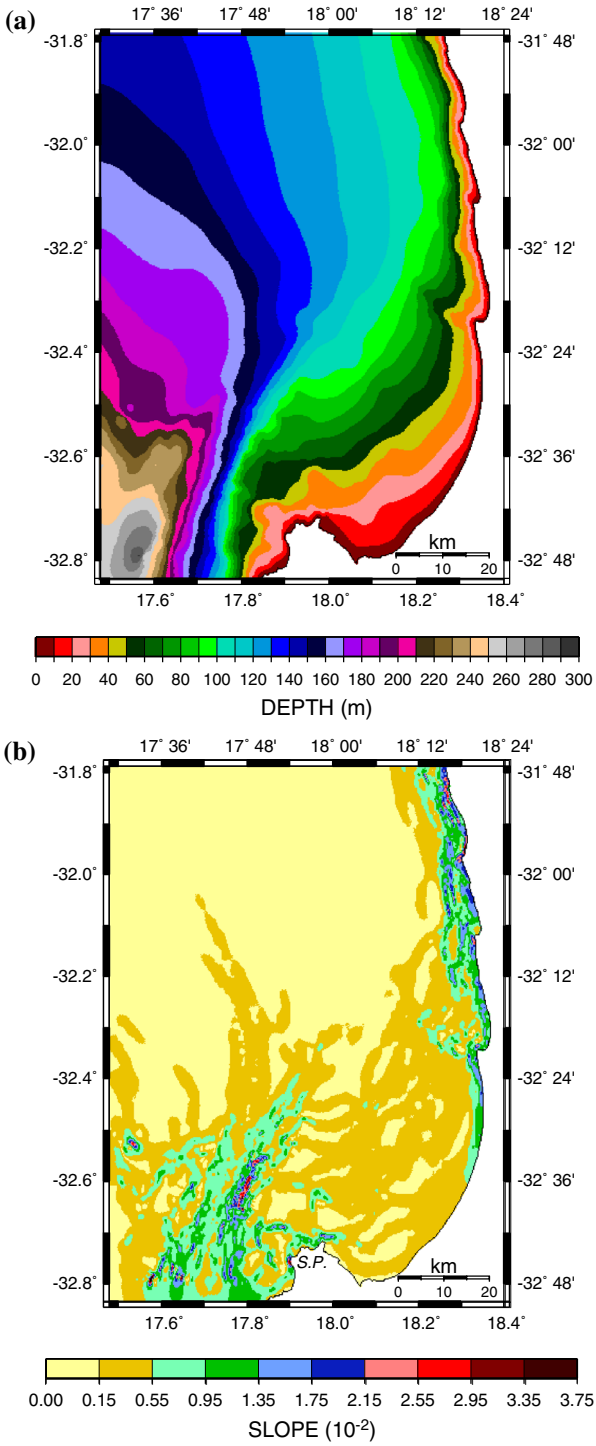

Fig. 4 **a** Bathymetry of St. Helena's Bay, *color*-coded at 10-m intervals. Adapted from Marine Geoscience Unit, Council of Geoscience. **b** Dataset of **a**, *color*-coded according to the slope of the ocean floor (in units of 10^{-2}). Note the canyon, approximately 20 km NW of Shelley Point (S.P.), where slopes reach 3 %

tsunamis (Okal et al. 2003, 2009), the amplitude of the negative trough and positive hump being $\eta_- = 7$ m and $\eta_+ = 3$ m, respectively, and the lever between them $l = 8$ km. The source is placed on the flank of the canyon, with the center of the trough at (32.605°S, 17.802°E), and the direction of the slide, N297°E, matching the local line of steepest descent of the bathymetry. The computation runs the MOST code (Titov and Synolakis 1998) which solves the nonlinear equations of hydrodynamics under the shallow-water approximation, using a finite differences integration through the method of alternating steps (Godunov 1959). MOST has been extensively validated through comparisons with laboratory and field data, per standard international protocols; full details can be found in Synolakis (2003). Our simulation uses a time step of 1 s and is run for 1 h.

In the absence of an adequate topographic database, the computation is stopped at a water depth of 1.5 m. Accordingly, the absolute values of the simulations (which at any rate are directly related to the arbitrary values of $\eta_\pm$ selected for the source) should not be compared directly to the values reported in Table 1. However, this methodology allows a comparison between the *relative* amplitudes predicted along various segments of the coastline. Note also that the evolving landscape along the sandy portions of the coastline in the past 40 years would in any case prevent a pertinent modeling of absolute run-up.

Results are presented on Fig. 5 in the form of a regional map of the maximum amplitude of the oscillation triggered by the landslide. Our simulation predicts a nearly constant amplitude (between 1 and 2 m) along most of the eastern shore of St. Helena Bay, between latitude 32.45°S, i.e., 25 km north of Dwarskersbos, and 32.77°S, at Velddrif, with a small local maximum to the south of Dwarskersbos. In addition, Fig. 6 plots time series of wave amplitudes at six virtual gauges shown as bull's eye symbols in Fig. 5. We note that the amplitudes simulated at Dwarskersbos do not stand out as significantly larger than on the neighboring beaches, especially at Brandhuis, where our witness indicated that there was no detectable wave action in 1969. Also, and expectedly, our simulation predicts much larger amplitudes (by a factor of 3) on the western side of Shelley Point promontory, reaching an offshore value of more than 4 m at Duikers Island, which would almost certainly have resulted in damage along the shore line, that should have been detected in the hours or days following the event.

We have also verified that our results (most importantly the similarity in simulated amplitudes at Dwarskersbos and Brandhuis) are not changed appreciably when altering the parameters of the source while keeping it in the canyon. The only other locations which could legitimately support an underwater landslide would be the steep cliffs in the neighborhood of Elands Bay or Lamberts Bay, which would result in a concentration of the largest amplitudes at those northern locations, rather than in St. Helena's Bay including at Dwarskersbos.

In conclusion, we discard a landslide as a source of the 1969 tsunami in Dwarskersbos, since it cannot explain the fundamental patterns of the survey, when positioned at the only regional sites physically capable of supporting it.

6.3 A resonant wave of meteorological origin

6.3.1 Background: meteo-tsunamis

In trying to identify a different mechanism for the generation of the 1969 Dwarskersbos wave, we note many instances of reported waves which can be generally regarded as anomalous, because their amplitude is unexpectedly large, and they occur independently of

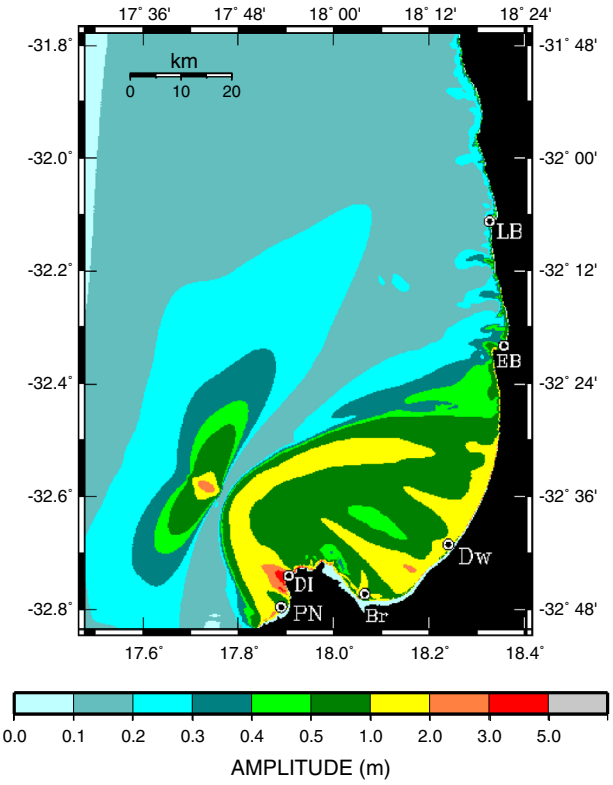

Fig. 5 Result of hydrodynamic simulation for the dipolar source located in the canyon identified on Fig. 4. The field is color-coded according to the maximum amplitude reached by the wave during a 1 h window. Bull's eye symbols identify six virtual gauges located off Dwarskersbos (Dw), Elands Bay (EB), Lamberts Bay (LB), Brandhuis (Br), Duikers Island (DI) and Paternoster (PN)

an identifiable tectonic source. The term "freak" or "rogue" wave is usually reserved for large amplitude waves observed in ocean basins, as reviewed recently by Kharif et al. (2009). By contrast, the development of waves of significant amplitudes along coastlines is most often the result of the resonance of coastal structures such as bays and harbors, with typical scales on the order of one to a few kilometer. This phenomenon leads to "harbor oscillations" or "seiches," the latter term being in principle reserved for the oscillation of an enclosed basin (Rabinovich 2009).

In the absence of an identifiable tectonic source for observed large water waves, their origin must be sought in a form of coupling between the oceanic column and the atmosphere, and the resulting phenomenon is generally referred to as a "meteo-tsunami," a term introduced by Nomitsu (1935), Defant (1960), and more recently Monserrat et al. (1991), and Rabinovich and Monserrat (1996, 1998). Note that the origin of the energy of "meteo-tsunamis" lies in the planet's weather system, and as such, is eventually traceable to solar radiation, rather than in the plate tectonics system of the dynamic Earth for earthquake tsunamis, or gravitational potential energy for landslide ones, both of which are eventually traceable to the Earth's internal engine, i.e., the slow release of its primordial heat, resulting from its accretion from the solar nebula.

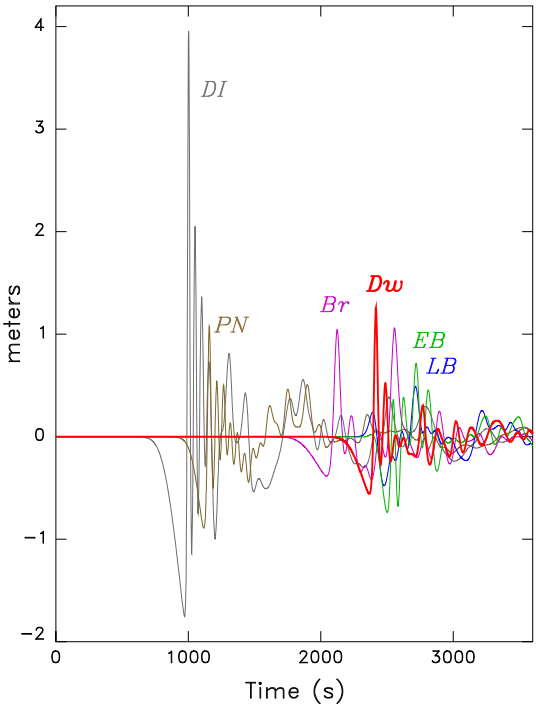

Fig. 6 Time series of the dipolar simulation at the six virtual gauges. Note that the Dwarskersbos trace does not stand up as significantly greater than Brandhuis or even Elands Bay

In order for meteo-tsunamis to reach significant amplitudes, the coupling between atmosphere and ocean must become resonant. In many instances, this resonance can be attributed, at least in part, to oscillations in a bay or harbor, as in the case of the "rissaga" [recess] phenomenon in the Balearic Islands, notably at Ciutadella Harbor, Menorca (Monserrat et al. 1991). However, resonance can also take place in the absence of a closed (or weakly open) coastal bay or harbor (and hence along a largely linear coastline such as the eastern shore of St. Helena Bay in the vicinity of Dwarskersbos), when the presence of a very shallow shelf allows a match between the speed of the meteorological disturbance and the velocity of long waves propagating in the ocean under the shallow-water approximation ($c = \sqrt{gh}$). This effect, known as "Proudman resonance," was investigated theoretically by Proudman (1929), and described, albeit for coastlines more irregular than at Dwarskersbos, e.g., along the Adriatic Sea by Šepić et al. (2009), the Western coast of Kyushu, Japan in 1979 by Hibiya and Kajiura (1982) and again in 2009 by Tanaka (2010), and most recently at Boothbay, Maine, by Vilibić et al. (2014).

One of the earliest cases for which a quantitative model of meteo-tsunami generation was proposed was the episode of June 26, 1954 in Lake Michigan, when an abrupt increase in the level of the lake, reaching a maximum of 3 m, resulted in at least seven casualties in the Chicago area, during a summer day of otherwise calm weather. Noting that the 1954 wave developed in the wake of a strong atmospheric pressure jump of 3,000 dyn/cm^2 (3 mbar) moving over the lake at an exceptional speed of 30 m/s (66 mph), Ewing et al. (1954) quickly proposed that the wave was due to a resonance between the wind speed and the natural velocity of gravity waves traveling in the lake under the shallow-water approximation. They identified a zone $\sim$60 km long where the depth of the lake (on the average 270 ft or 82 m) would translate into an appropriate wave velocity (28 m/s). Platzman (1958) later carried out

a hydrodynamic simulation of the response of the southern part of Lake Michigan to forcing by the passage of an atmospheric pressure discontinuity, which produced an acceptable model of the wave, as recorded on a tidal instrument in downtown Chicago. This model was essentially confirmed through more sophisticated recent computations by Wu et al. (2012). Note, however, that the 1954 wave was observed over a large section of Lake Michigan, extending at least 100 km to the shores of Indiana. From a more qualitative standpoint, Donn (1959) also applied a similar approach to the case of a more widespread system of exceptional surges observed throughout the Great Lakes on May 05, 1952.

Another well-studied case is that of the Daytona Beach, Florida wave of July 04, 1992 (Thieke et al. 1993). In that instance, a wave described by witnesses as having an offshore amplitude as high as 6 m, broke upon shoaling, creating a run-up of 3 m and an inundation on the order of 150 m. Miraculously, it caused no fatalities, but resulted in damage to vehicles present on the beach. The Daytona Beach wave was observed along a 30 km stretch of coastline, but its maximum run-up was distributed over only 6 km, leading to an aspect ratio $I_2 = 2.3 \times 10^{-4}$, which approaches that at Dwarskersbos. Using a wealth of meteorological data, Churchill et al. (1995) later showed that the wave could be interpreted as resulting from resonant coupling between a squall line propagating across Florida with a pressure jump of ~ 2 mbar across its front, and an ocean gravity wave traveling along the shallow continental edge structure. The resonance occurred as the wind speeds measured in the squall (25 knots or 13 m/s) coincided with the gravity wave speed for an average water depth of 17 m. In both the Chicago and Daytona Beach cases, the shoreline was essentially straight, which rules out the oscillation of a bay or harbor as the origin of the resonance. A review of more instances of probable meteo-tsunamis on the eastern shore of the USA has recently been given by Pasquet et al. (2013).

Other instances of waves observed on shorelines, of a most probable meteorological origin include, among others, the Sussex, England wave of July 20, 1929 (Proudman 1929), and the more recent event of June 27, 2011, observed from the Bay of Biscay to Cornwall (Tappin et al. 2012); the Western Black Sea event of May 07, 2007 (Vilibić et al. 2010), even though a landslide origin has also been advocated (Ranguelov et al. 2008); and a series of surges correlated to extreme atmospheric conditions along the coast of Western Australia (Wijeratne and Pattariatchi 2013). Finally, although less well documented, the case of the western Algeria wave which killed 12 people on four beaches in the vicinity of Mostaganem on August 03, 2007, shares many characteristics with the 1954 Chicago event, suggesting a similar origin (N.-E. Taibi, pers. comm., 2013).

6.3.2 Modeling of the Dwarskersbos wave

In this framework, we follow Platzman's (1958) approach to suggest a model of meteorological generation of the 1969 Dwarskersbos tsunami. Based on a concept initially presented by Chrystal (1908), and following Proudman (1953, pp. 295–302), Platzman solves the hydrodynamic equations of motion in their depth-integrated, shallow-water form

$$\frac{\partial \mathbf{M}}{\partial t} = D \cdot (\mathbf{F} - g\,\mathbf{grad}\ h) \tag{1}$$

$$\frac{\partial h}{\partial t} = -\mathrm{div}\,\mathbf{M} \tag{2}$$

where h is the (vertical) amplitude of the deformation of the ocean surface, D the local depth of the unperturbed ocean column ($|\,h\,| \ll D$), $\mathbf{M}$ the integral of the horizontal velocity field $\mathbf{v}$ over the oceanic column

$$\mathbf{M} = \int_{-D}^{h} \mathbf{v} \cdot dz \tag{3}$$

and $\mathbf{F}$ represents the dynamic forcing of the ocean (of density ρ_w) by the gradient of pressure at its surface

$$\mathbf{F} = \frac{-1}{\rho_w} \cdot \mathbf{grad}\, P \tag{4}$$

the boundary conditions requiring simply that the normal component of $\mathbf{M}$ vanish at the shores.

Following Platzman (1958), we represent the pressure field of the squall by a ramp of amplitude Δp spread over a front of width L (in other words, its gradient in (4) is a boxcar of amplitude $\Delta p/L$), propagating in the azimuth ϕ at a speed C. We take $L = 5$ km, $\Delta p = 5$ mbar, $\rho_w = 1,020$ kg/m^3 and conduct a grid search over the kinematic parameters of the squall in the range C =10–30 m/s; ϕ = N50 − 130°E. Figures 7 and 8 show the results of our simulation for our preferred solution ($C = 18$ m/s; ϕ = N101°E).

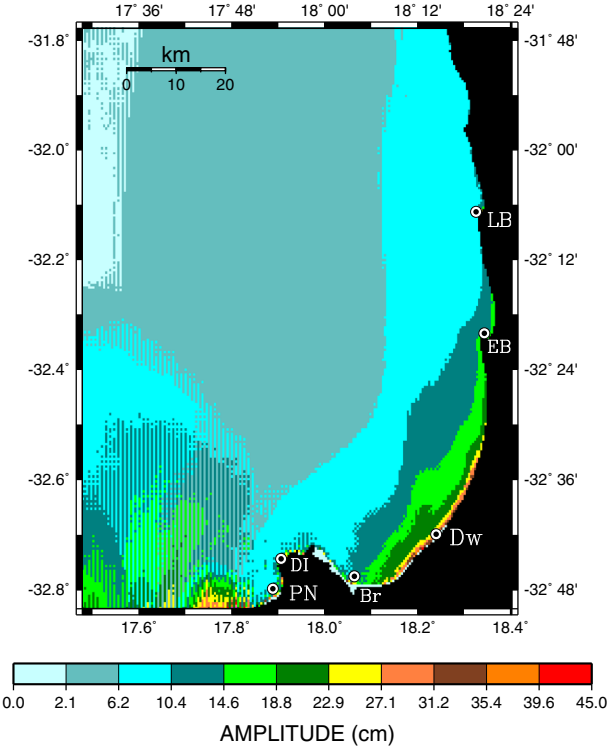

Fig. 7 Same as Fig. 5 for the case of a gravity wave coupled to a squall propagating at optimized velocity and azimuth. Note the concentration of the high wave amplitudes along the eastern shore of St. Helena Bay in the vicinity of Dwarskersbos

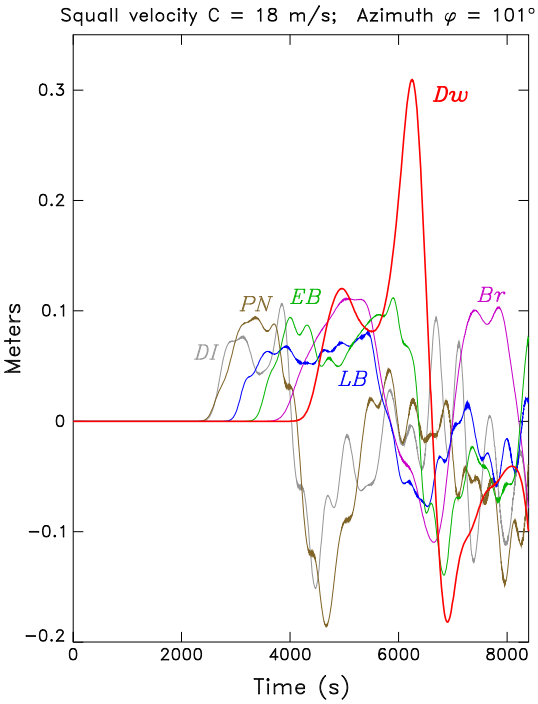

Fig. 8 Same as Fig. 6 for the squall-coupled gravity wave. Note that the time series at Dwarskersbos clearly stands out against those at the other locations

The fundamental result from these figures is the development of a line of strong amplitudes limited to the eastern shores of St. Helena Bay. In particular, Fig. 8 shows that the amplitude reached at the virtual gauge off Dwarskersbos is roughly three times larger than at all other locations, thus reproducing the main characteristic of our observations, namely the concentration of the wave at Dwarskersbos. This is in clear contrast to the case of the landslide simulations shown in Fig. 6. The proposed velocity of propagation C of the atmospheric front (18 m/s or 65 km/h) will coincide with that of shallow-water gravity waves for a depth D =33 m, which constitutes a reasonable average of the bathymetry in the first 20 km off the eastern shore of St. Helena Bay (Fig. 4). Any other segment of the coast features much steeper underwater slopes, rapidly leading to greater depths, which in turn would require much faster values of C to sustain resonance.

Our tests further indicate that lower values of C displace the locus of maximum amplitude to the south in the direction of the estuary of the Berg River, and conversely higher values of C displace it to the northeast. This simply illustrates a general deepening of the shelf from SW to NE along the eastern shore of St. Helena Bay (Fig. 4a). Similarly, a rotation of the azimuth of propagation of the squall ϕ displaces the lobe of the wave across the Dwarskersbos beach. The best results, focusing the wave on Dwarskersbos and maintaining a ratio of at least 3 between the amplitudes at Dwarskersbos and at the runner-up virtual gauge, are obtained for ($16 \leq C \leq 20$ m/s) and ($92^\circ \leq \phi \leq 110^\circ$), and thus, our solution for the kinematic parameters of the squall can be given as ($C = 18 \pm 2$ m/s; $\phi = 101 \pm 9^\circ$).

This simple computation does not propagate the wave over the shoreline, and thus should not be interpreted in terms of a comparison with the absolute run-up amplitudes measured during our survey. Indeed, the factor of ~ 8 between the maximum run-up

reported at Dwarskersbos and the maximum amplitude in the open water compares favorably with that of ~ 6 reported by Churchill et al. (1995) in their study of the Daytona Beach event. Also, the smaller value of the aspect ratio I_2 at Daytona Beach could be due to a propagation of the squall in a direction more parallel to the coastline.

7 Conclusion

Our on-site survey of the Dwarskersbos tsunami, conducted 41 years after its occurrence, confirms the extreme concentration of the observable run-up (maximum amplitude 2.9 m) along a stretch of coastline less than 2 km in length. Such characteristics rule out its generation by an earthquake (which at any rate should have been felt by the local population). A landslide source also can be eliminated since numerical simulation using a source at the only nearby location with a sufficient slope fails to reproduce the concentration of wave energy along the Dwarskersbos shoreline.

Rather, we obtain a satisfactory match of the distribution of run-up along the coast by simulating the interaction of a meteorological squall propagating at 18 m/s in the azimuth N101°E with gravity waves in the shallow waters immediately west of the shoreline, using the analytical formulation of Proudman (1953).

The 1969 Dwarskersbos event thus constitutes one more example of meteo-tsunamis expressing a subtle coupling between atmosphere and oceans. This is made possible by exceptionally slow velocities for shallow-water gravity waves in beaches featuring extended shallow bathymetry, and propagation of pressure fronts at velocities unusually fast for meteorological events at the Earth's surface. Such circumstances bridge the usual gap between the speeds of the atmospheric and oceanic perturbations, resulting in the possible resonant transfer of energy from the former system to the latter.

While the generation of meteo-tsunamis requires exceptional circumstances, a growing number of studies have recently documented, interpreted, and modeled these phenomena, which must be considered as potential sources of hazard along beaches featuring extended shallow bathymetry. Our study resolves the enigma of the 1969 Dwarskersbos wave by showing that it indeed belongs to the family of meteo-tsunamis, providing additional evidence of vulnerability to their hazard along a geographically diverse range of coastlines, and in particular in the absence of traditional sources of resonance, such as bays and harbors.

Acknowledgments We thank Wilhelm van Zyl of the Marine Geoscience Unit, Council of Geoscience, for a digitized map of the bathymetry of St. Helena Bay, and Mr. Theuns Smit of Dwarskersbos for access to a 1967 land-surveyor's map of the future town layout. Mr. Nikos Kalligeris helped in the initial aspects of the landslide simulation. Discussions are also acknowledged with Dr. Nasr-Eddine Taibi during the RASMER meeting in Zeralda, Algeria, in June 2013. Constructive comments on the original version of the paper by Editor Alexander Rabinovich and two anonymous reviewers are gratefully acknowledged. We are grateful to Emily Wolin for help with the final production of the manuscript, especially Fig. 3.

References

Ben-Avraham Z, Smith G, Reshef M, Jungslage E (2002) Gas hydrate and mud volcanoes on the southwest African continental margin off South Africa. Geology 30:927–930

Chrystal G (1908) An investigation of the seiches of Loch Earn by the Scottish lake survey, part V: mathematical appendix on the effect of pressure disturbances upon the seiches in a symmetric parabolic lake. Trans R Soc Edinb 46:499–517

Churchill DD, Houston SH, Bond NA (1995) The Daytona Beach wave of 3–4 July 1992: a shallow water gravity wave forced by a propagating squall line. Bull Am Meteorol Soc 76:21–32
Defant A (1960) Physical oceanography, vol 2. Pergamon, Oxford, p 234
Donn WL (1959) The Great Lakes storm surge of May 5, 1952. J Geophys Res 64:191–198
Ewing M, Press F, Donn WL (1954) An explanation of the Lake Michigan wave of 26 June 1954. Science 120:684–686
Geller RJ (1976) Scaling relations for earthquake source parameters and magnitudes. Bull Seismol Soc Am 66:1501–1523
Godunov SK (1959) Finite difference methods for numerical computations of discontinuous solutions of the equations of fluid dynamics. Mat Sb 47:271–295
Hartnady CJH, Brundrit G, Hunter I, Luger I, Saunders I, Wonnacott R (2009) The Cape West Coast tsunami of 20–21 August 2008. Proceedings of Gen. Assemb. Intl. Assoc. Seism. Phys. Earth Inter., Cape Town [abstract]
Hibiya T, Kajiura K (1982) Origin of "Abiki" phenomenon (kind of seiches) in Nagasaki Bay. J Oceanogr Soc Jpn 38:172–182
Keyser AW (1974) Some macroscopic observations in the meizoseismal area of the Boland earthquake of 29th September 1969. Counc Geosci Seismol Ser 4:18–25
Kharif C, Pelinovsky E, Slunyaev A (2009) Rogue waves in the ocean. Springer, Heidelberg, 216 pp
Monserrat S, Ibberson A, Thorpe AJ (1991) Atmospheric gravity waves and the "rissaga" phenomenon. Q J R Meteorol Soc 117:553–570
Monserrat S, Vilibić I, Rabinovich AB (2006) Meteotsunamis: atmospherically induced destructive ocean waves in the tsunami frequency band. Nat Haz Earth Syst Sci 6:1035–1051
Nomitsu T (1935) A theory of tsunamis and seiches produced by wind and barometric gradient. Mem Coll Sci Imp Univ Kyoto Ser A 18:201–214
Okal EA, Synolakis CE (2004) Source discriminants for near-field tsunamis. Geophys J Int 158:899–912
Okal EA, Synolakis CE, Fryer GJ, Heinrich P, Borrero JC, Ruscher C, Arcas D, Guille G, Rousseau D (2002) A field survey of the 1946 Aleutian tsunami in the far field. Seismol Res Lett 73:490–503
Okal EA, Plafker G, Synolakis CE, Borrero JC (2003) Near-field survey of the 1946 Aleutian tsunami on Unimak and Sanak Islands. Bull Seismol Soc Am 93:1226–1234
Okal EA, Synolakis CE, Uslu B, Kalligeris N, Voukouvalas E (2009) The 1956 earthquake and tsunami in Amorgos, Greece. Geophys J Int 178:1533–1554
Pasquet S, Vilibić I, Šepić J (2013) A survey of strong high-frequency sea level oscillations along the U.S. East Coast between 2006 and 2011. Nat Hazards Earth Syst Sci 13:473–482
Platzman GW (1958) A numerical computation of the surge of 26 June 1954 on Lake Michigan. Tech. Rept. Nr. 1, U.S. Weather Bureau, Univ. Chicago, 46 pp
Proudman J (1929) The effect on the sea of changes in atmospheric pressure. Mon Not R Astr Soc Geophys Supp 2:197–209
Proudman J (1953) Dynamical oceanography. Methuen, London, 409 pp
Rabinovich AB (2009) Seiches and harbor oscillations. In: Kim YC (ed) Handbook of coastal and ocean engineering. World Scientific Publishing, Singapore, pp 193–244
Rabinovich AB, Monserrat S (1996) Meteorological tsunamis near the Balearic and Kuril Islands: descriptive and statistical analysis. Nat Hazards 13:55–90
Rabinovich AB, Monserrat S (1998) Generation of meteorological tsunamis (large amplitude seiches) near the Balearic and Kuril Islands. Nat Hazards 18:27–55
Ranguelov B, Tinti S, Pagnoni G, Tonini R, Zaniboni F, Armigliato A (2008) The non-seismic tsunami observed in the Bulgarian Black Sea on 7 May 2007: was it due to a submarine landslide? Geophys Res Lett 35(18):L18613, 5 pp
Šepić J, Vilibić I, Belušić D (2009) The source of the 2007 Ist meteo-tsunami (Adriatic Sea). J Geophys Res 114(C3):C03016, 14 pp
Synolakis CE (2003) Tsunami and seiche. In: Chen W-F, Scawthron C (eds) Earthquake engineering handbook. CRC Press, Boca Raton, pp 9_1–9_90
Synolakis CE, Okal EA (2005) 1992–2002: perspective on a decade of post-tsunami surveys. In: Satake K (eds) Tsunamis: case studies and recent developments. Adv. Natur. Technol. Hazards, vol 23, pp 1–30
Synolakis CE, Bardet J-P, Borrero JC, Davies HL, Okal EA, Silver EA, Sweet S, Tappin DR (2002a) The slump origin of the 1998 Papua New Guinea tsunami. Proc R Soc (Lond) Ser A 458:763–789
Synolakis CE, Yalçıner AC, Borrero JC, Plafker GL (2002b) Modeling of the November 3, 1994 Skagway, Alaska tsunami. In: Wallendorf L, Ewing L (eds) Solutions to coastal disasters, Edited by Amer. Soc. Civil Eng., pp 915–927
Tanaka K (2010) Atmospheric pressure-wave bands around a cold front resulted in a meteo-tsunami in the East China Sea in February 2009. Nat Hazards Earth Syst Sci 10:2599–2610

Tappin DR, Sibley A, Horsburgh K, Daubord C, Cox D, Long D (2012) The English Channel tsunami of 27 June 2011—a probable meteorological source. Eos Trans Am Geophys Un 93(53):NH21D-05 [abstract]

Thieke RJ, Dean Thieke RJ, Dean RG, Garcia AW (1993) The Daytona Beach "large wave" event of 3 July 1992. In: Proceedings of 2nd international symposium ocean wave measurement and analysis, Amer. Soc. Civil Eng., New Orleans, pp 45–60

Titov VV, Synolakis CE (1998) Numerical modeling of tidal wave runup. J Wtrwy Port Coast Eng B124:157–171

Vilibić I, Horvath K, Strelec Mahović N, Monserrat S, Marcos M, Amores A, Fine I (2014) Atmospheric processes responsible for generation of the 2008 Boothbay meteo-tsunami. Nat Hazards (in press)

Vilibić I, Šepić J, Ranguelov B, Mahović NS, Tinti S (2010) Possible atmospheric origin of the 7 May 2007 western Black Sea shelf tsunami event. J Geophys Res 115(C7):C07006 12 pp

Wijeratne S, Pattariatchi C (2013) Meteo-tsunamis along the west Australian coastline. In: Proceedings of joint Assemb. Intl. Assoc. Seismol. Phys. Inter. Earth, Göteborg, 22–26 Jul. 2013, SP1S4.06 [abstract]

Wu C, Bechle A, Schwab DJ, Anderson EJ, Roebber PJ (2012) Meteo-tsunamis in Lake Michigan. Eos Trans Am Geophys Un 93(53):NH21D-04 [abstract]